Effect of stimulated processes on the Hanle signal. Investigation of the total signal intensity

F. A. Lomaya and A. A. Panteleev

Troitsk Institute of Innovative and Thermonuclear Research, 142092 Troitsk, Moscow Region, Russia
(Submitted 5 December 1994)
Zh. Éksp. Teor. Fiz. **108**, 23–35 (July 1995)

We study the effects of absorption (amplification) and four-wave mixing on the total fluorescence intensity of atoms excited by a monochromatic wave of arbitrary intensity in a constant magnetic field. We study scattering by optically thick and optically thin atomic beams, and by an optically thin beam in a high-Q cavity. These investigations are carried out for the $J=0\rightarrow J=1$ transition with the pump wave propagating perpendicular to the magnetic field (Voigt geometry). Differences in the description of the Hanle effect in the Voigt and Faraday (pump wave propagation parallel to the magnetic field parallel) geometries are studied. The characteristics of the Hanle effect for the transition $J=1\rightarrow J=0$ are also discussed.

1. INTRODUCTION

The depolarization of radiation scattered by atoms in a magnetic field was discovered by Hanle 70 years ago,[1,2] and it is the subject of many theoretical and experimental investigations (see Ref. 3). This phenomenon makes it possible to measure efficiently the constants of spectral lines in gases,[3] it is used to study the properties of the interaction of radiation with matter,[4,5] and it is closely related to the transfer of polarized radiation[6] and other questions in optics and spectroscopy.

Most theoretical investigations of the Hanle effect have been performed for low (nonsaturating) intensities of the radiation exciting the atoms. In Refs. 7 and 8 we presented a description unconstrained by this approximation, i.e., one that is valid for arbitrary radiation intensities. The investigation was performed for the Voigt geometry, in which the magnetic field is perpendicular to the propagation direction of the exciting radiation and its linear polarization vector (see Fig. 1). It was assumed that the pump wave is monochromatic and is scattered by an atomic beam, so that transitions occur between the ground state with $J=0$ and the excited states with $J=1$. In this geometry, the Hanle signal is determined by radiation that is linearly polarized in the x direction and scattered in the y or z direction. In Ref. 7, spectra of the Hanle signal for a pump wave scattered by an optically thin atomic beam were investigated. In this case the signal is determined by the fluorescence of the atoms, and it was shown, just as in the case of Mollow's resonance fluorescence spectrum,[9] that the spectrum of the Hanle signal contains both an elastic (coherent) component and an inelastic (shifted) component. In strong (saturating) fields, the inelastic component, whose spectrum contains up to seven components, is dominant. In Ref. 8, the effect of induced processes on the spectrum of the Hanle signal for pump-wave scattering by optically thick and optically thin atomic beams passing through a high-Q cavity was investigated. It was shown that the interference terms arising in the description of the Hanle effect can be regarded as a type of four-wave interaction.

In many experimental investigations of the Hanle effect, it is not the spectrum of the scattered radiation that is studied, but rather the total intensity of the spectrum, i.e., the integral over the spectrum. The present paper is a continuation of the investigations initiated in Ref. 8, and is devoted to a study of the effects of stimulated processes on the total intensity of the Hanle signal.

Just as in Ref. 8, two model experimental situations (see Fig. 1) are studied: scattering of the pump wave by an optically thin beam in a cavity (not shown in Fig. 1), and by an optically thick atomic beam. In addition, we discuss the properties of the forward-scattered radiation and the differences in the description of the Hanle effect between the Voigt geometry studied in Refs. 7 and 8 and the Faraday geometry (in which the pump wave propagates parallel to the magnetic field). The $J=0\rightarrow J=1$ atomic transition is the simplest atomic system in which the Hanle effect is observed, and it corresponds to a V-type interaction between the polarized radiation and the atoms. It is also of interest to study the properties of the Hanle effect for the $J=1\rightarrow J=0$ transition, which corresponds to a Λ-type interaction. In the last section, we consider how results obtained in Refs. 7 and 8 change when our description is applied to this transition. The experimental and theoretical results presented in Ref. 5 are also discussed.

2. DESCRIPTION OF THE HANLE EFFECT

The results of Refs. 7, 8 and 10, which were obtained on the basis of the Scully–Lamb atom–photon density matrix formalism[11] in the rotating-wave and dipole- interaction approximations, are used to describe the Hanle effect.

The correlation functions that arise in the description of the scattered radiation[7,8] are $n_\sigma=\langle a_\sigma^+ a_\sigma\rangle=\langle a_\sigma^+ a_\sigma P\rangle$ and $\langle a_{\sigma'}^+ a_\sigma\rangle=\langle a_{\sigma'}^+ a_\sigma P\rangle$ $(\sigma\neq\sigma')$. Here P is the photon density operator and a_σ^+ and a_σ are creation and annihilation operators for photons with wave vector $\mathbf{k}_\sigma$ and frequency ω. The index σ indicates an interaction with the corresponding σ transition of the atomic subsystem. For circularly polarized photons a plus sign in the index indicates left-hand polariza-

 1063-7761/95/070012-07$10.00

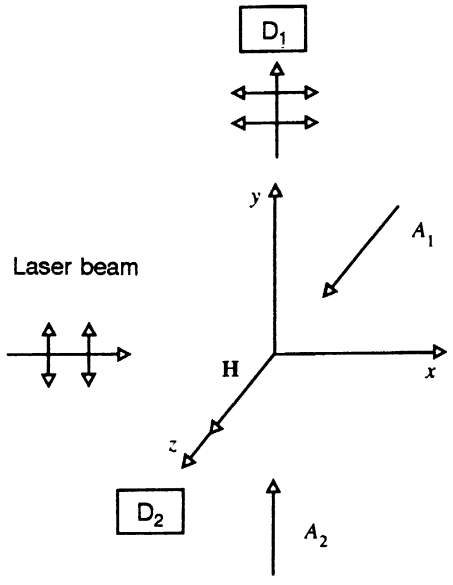

FIG. 1. Possible experimental layout for observing the Hanle effect. The vector **H** specifies the direction of the magnetic field, A_1 and A_2 are atomic beams, and D_1 and D_2 are scattered-radiation detectors.-

tion and a minus sign in the index indicates right- hand polarization. The quantity n_σ determines the occupation numbers of photons with the wave vector $\mathbf{k}_\sigma$. The existence of the correlation functions $\langle a^+_{\sigma'} a_\sigma \rangle$ is associated with the coherence that the pump wave introduces into the given system, and makes it possible to describe the interference effects that are important, particularly in the Hanle effect.

The equations of motion for the photon occupation numbers and for the quantum correlation functions of photons with different polarization take the form[7,8]

$$\frac{d}{dt}\mathbf{n}=\mathbf{Dn}+\mathbf{A}, \tag{1}$$

where

$$\mathbf{n}=\begin{pmatrix} n_+ \\ n_- \\ \langle a^+_- a_+ \rangle \\ \langle a^+_+ a_- \rangle \end{pmatrix}, \quad \mathbf{A}=\begin{pmatrix} \mathscr{A}_{++} \\ \mathscr{A}_{--} \\ \mathscr{A}_{-+} \\ \mathscr{A}_{+-} \end{pmatrix},$$

$$\mathbf{D}=\begin{pmatrix} \alpha'_+ + \alpha'^*_+ & 0 & \beta^*_+ & \beta_+ \\ 0 & \alpha'_- + \alpha'^*_- & \beta_- & \beta^*_- \\ \beta^*_- & \beta_+ & \alpha'_+ + \alpha'^*_- & 0 \\ \beta_- & \beta^*_+ & 0 & \alpha'_- + \alpha'^*_+ \end{pmatrix}$$

Here $\mathscr{A}_{\sigma\sigma'}=A_{\sigma\sigma'}+A^*_{\sigma'\sigma}$, $\alpha'_\sigma=\alpha_\sigma-\omega/2Q$, $\alpha_\sigma=A_{\sigma\sigma}-B_{\sigma\sigma}$, and $\beta_\sigma=A_{\sigma\sigma'}-B_{\sigma\sigma'}$, and Q is the cavity quality factor for a given mode. In the case of radiative scattering in free space, the coefficient α' is replaced by α.

The coefficients A and B are defined in Refs. 7 and 8, and are functions of the frequency differences $\Delta_L=\omega_0-\omega_L$, and $\nu=\omega-\omega_L$, where ω_0 is the transition frequency and ω_L is the frequency of the monochromatic laser wave. They also depend on the spontaneous relaxation rate γ, the strength of the magnetic field, and the intensity of the pump wave. The influence of these factors is governed by the Larmor frequency Ω and the Rabi frequencies V_σ, respectively. Here $V_\sigma=-\mu_{\sigma 0}E_\sigma/2\hbar$, where $\mu_{\sigma 0}$ is the dipole matrix element for the $|0\rangle\rightarrow|\sigma\rangle$ transition (the vector $|0\rangle$ describes the lower state of the atom, while $|\sigma\rangle$ describes the upper state, which is $|+\rangle$ for $m_J=+1$ or $|-\rangle$ for $m_J=-1$); the sum of E_+ and E_- gives the intensity of the electric field of the pump wave. In the calculations we assume that $|V_+|=|V_-|=V$. The quantities $\mathscr{A}_{\sigma\sigma'}$ describe the spontaneous sources, whose properties were investigated in Ref. 9. The coefficients α and β characterize stimulated processes—radiative absorption and four-wave mixing—whose properties were investigated in Ref. 8.

The equations (1) make it possible to describe the Hanle effect, i.e., the effect of a magnetic field on the polarization characteristics of fluorescence in the system shown in Fig. 1. The Hanle signal is determined by the occupation numbers of photons with linear x-polarization, and the fluorescence spectrum is accordingly determined by $\mathscr{A}_x$. Using the relation between the Cartesian and circular unit vectors and the corresponding photon creation and annihilation operators, we obtain the following relations for the photon occupation numbers:

$$n_x=n_+ + n_- - \langle a^+_+ a_- \rangle - \langle a^+_- a_+ \rangle, \tag{2}$$

$$n_y=n_+ + n_- + \langle a^+_+ a_- \rangle + \langle a^+_- a_+ \rangle. \tag{3}$$

The x-polarized photons are observed along the y axis and the y-polarized photons are observed along the z axis (see Fig. 1). In the latter case, to avoid the Doppler effect, the atomic beam must be directed along the x axis.

The general expressions for the number $n_\parallel$ of photons that are linearly polarized in the plane containing the y axis and the vector **e**, and the number $n_\perp$ of photons whose linear polarization vector is orthogonal to this plane, take the form

$$n_\parallel=(n_+ + n_-)(1-\cos^2\theta\sin^2\varphi)+(\sin^2\theta-\cos^2\varphi\cos^2\theta) \times(\langle a^+_+ a_- \rangle + \langle a^+_- a_+ \rangle)+i\sin 2\theta\cos\varphi(\langle a^+_+ a_- \rangle - \langle a^+_- a_+ \rangle), \tag{4}$$

$$n_\perp=(n_+ + n_- - \langle a^+_+ a_- \rangle - \langle a^+_- a_+ \rangle)\cos^2\theta. \tag{5}$$

Here the vector **e** determines the direction of photon scattering, θ is the angle between **e** and the y axis, and φ is the angle between the projection of **e** on the xz plane and the x axis.

For optically thin media, in which stimulated processes can be neglected, it follows from Eq. (1) that $n_\sigma \propto \mathscr{A}_{\sigma\sigma}$, $\langle a^+_\sigma a_{\sigma'} \rangle \propto \mathscr{A}_{\sigma\sigma'}$. Substituting these relations into Eqs. (2) and (3), we obtain

$$n_x \propto \mathscr{A}_x = \mathscr{A}_{++} + \mathscr{A}_{--} - \mathscr{A}_{+-} - \mathscr{A}_{-+}, \tag{6}$$

$$n_y \propto \mathscr{A}_y = \mathscr{A}_{++} + \mathscr{A}_{--} + \mathscr{A}_{+-} + \mathscr{A}_{-+}. \tag{7}$$

These spectra were investigated in detail in Ref. 7.

The total intensity of the Hanle signal is given by

$$S_x \propto N_x = \int n_x \, d\nu. \tag{8}$$

Using the properties of the $\mathscr{A}_{\sigma\sigma'}$,

$$\int \mathscr{A}_{\sigma\sigma'}\, d\nu \propto \rho_{\sigma\sigma'}, \tag{9}$$

we obtain

$$S_x \propto \rho_{++}+\rho_{--}-\rho_{+-}-\rho_{-+}, \tag{10}$$

$$S_y \propto \rho_{++}+\rho_{--}+\rho_{+-}+\rho_{-+}. \tag{11}$$

Here $\rho_{\sigma\sigma'}$ are the components of the atomic density matrix.[8] For $\sigma=\sigma'$ they determine the populations of the excited states, and for $\sigma \neq \sigma'$ they determine the coherence between them. The components $\rho_{0\sigma}$ determine the coherence between the excited and ground states. We find the components of the atomic density matrix from the steady-state solution of Eq. (4) in Ref. 8. The relations (10) and (11) are investigated by Avan and Cohen- Tannoudji in Ref. 12.

It should be noted that since the lower level in our atomic subsystem corresponds to the ground state, two components can be identified in the fluorescence spectra: an elastic, or unshifted, component $\mathscr{A}^{\rm el}_{\sigma\sigma'}$ proportional to $\delta(\nu)$, and an inelastic component $\mathscr{A}^{\rm inel}_{\sigma\sigma'}$, which describes scattering with a change in photon frequency. The expressions for $\mathscr{A}^{\rm el}_x$ and $\mathscr{A}^{\rm el}_y$ take the form[7]

$$\mathscr{A}^{\rm el}_x = 2\pi N|g_+\rho_{0+}-g_-\rho_{0-}|^2\delta(\nu), \tag{12}$$

$$\mathscr{A}^{\rm el}_y = 2\pi N|g_+\rho_{0+}+g_-\rho_{0-}|^2\delta(\nu), \tag{13}$$

where N is the number of scattering atoms, $\delta(\nu)$ is the Dirac delta function, and the g_σ are coupling constants.

3. EFFECT OF STIMULATED PROCESSES ON THE TOTAL INTENSITY OF THE HANLE SIGNAL

3.1. Effect of the cavity

We consider the experimental situation depicted in Fig. 1. We assume that the scattering system is located in a high-Q Fabry–Perot cavity oriented along the y or z axis. The scattered radiation is selected by the spectral modes of the cavity and then measured with an external detector. We assume that the width of the intracavity modes is large enough compared to the total width of the fluorescence spectra that it does not affect the form of the modes. When the atoms are irradiated by a laser, the number of photons rises to some steady-state value. This state is described by the steady-state solution of Eq. (1):

$$\mathbf{n}=-\mathbf{D}^{-1}\mathbf{A}. \tag{14}$$

Substituting this solution into Eq. (2) and (3), we obtain expressions for the numbers of photons n_x and n_y. The effect of a cavity on the spectra of these quantities is investigated in Ref. 8. The total intensity of the Hanle signal is determined by (8). Note that the spontaneous sources in Eq. (2) contain two components, elastic and inelastic. We therefore represent N_x in the form

$$N_x = N_x^{\rm el}+N_x^{\rm inel}, \tag{15}$$

where the first term is calculated with the spontaneous sources $\mathscr{A}^{\rm el}_{\sigma\sigma'}$ and the second is calculated with $\mathscr{A}^{\rm inel}_{\sigma\sigma'}$.

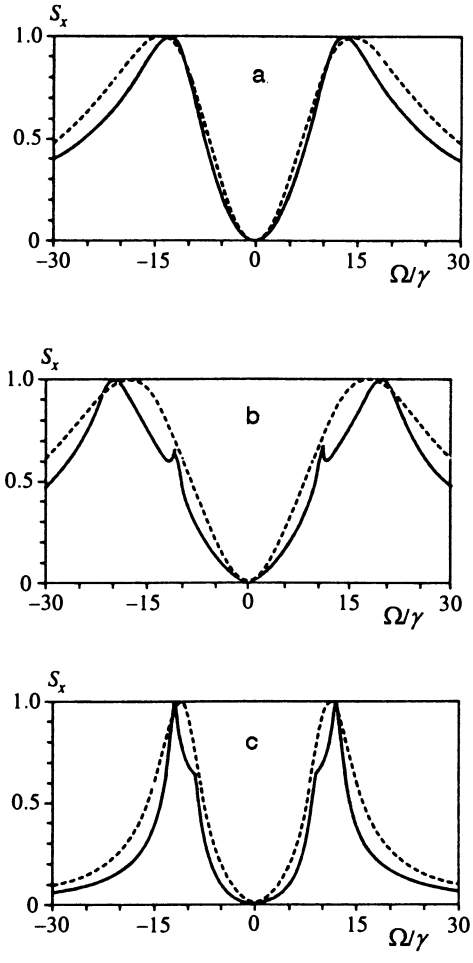

FIG. 2. S_x as a function of Ω (magnitude of the magnetic field) for a high-Q cavity (solid curve, $q=0.05$) and a low-Q cavity (dashed curve, $q\gg 1$) for various parameter values: a) $V/\gamma=10$, $\Delta_L=0$; b) $V/\gamma=10$, $\Delta_L/\gamma=10$; c) $V/\gamma=3$, $\Delta_L/\gamma=10$. The peak values of S_x are normalized to unity.

Since $\mathscr{A}^{\rm el}_{\sigma\sigma'} \propto \delta(\nu)$, $N_x^{\rm el}$ can be determined quite simply after the corresponding integration has been performed. For the present paper, the $N_x^{\rm inel}$ were calculated numerically with a personal computer.

Figure 2 displays S_x as a function of the saturating magnetic field in a high- Q cavity, as given by Eqs. (2), (8), and (14) (solid curve), and in a low-Q cavity (dashed curve, $q\gg 1$) as given by Eq. (10), which corresponds to scattering of radiation in free space. Both results were obtained with saturating pump-wave intensities ($V\gg\gamma$). Here $q=\omega/Qk_0$, where k_0 is the unperturbed radiative absorption rate at line center ($E_\sigma=\Omega=\Delta_L=0$). In experimental investigations of the total intensity S_x of the Hanle signal, one typically studies the dependence of the line profile on the magnitude of the magnetic field. For convenience in comparing the profiles in Fig. 2, we therefore normalize the peak line values to unity.

One can see from Fig. 2 that the strongest effect of a high value of Q on the line profile is observed at $V\sim\Delta_L$, and that the effect is modest at small ($\Delta_L\ll V$) or large ($\Delta_L\gg V$) mismatches. Our analysis shows that in weak fields ($V\ll\gamma$), the cavity Q has only a minor effect on the line profile and total intensity of the Hanle signal.

3.2. Propagation effects

We now consider the scattering of the pump wave by an optically thick atomic beam (no cavity). The propagation of the scattered radiation is described by the system of equations (1). In the form given here, this system affords us no opportunity for a convenient analytic solution. We therefore write the system in a more symmetric form, for which we introduce the matrix

$$\Sigma=\begin{vmatrix} n_+ & \langle a_-^+ a_+\rangle \\ \langle a_+^+ a_-\rangle & n_- \end{vmatrix}. \tag{16}$$

Equation (2) then takes the form

$$\frac{d}{dt}\Sigma=\mathbf{K}\Sigma+\Sigma\mathbf{K}^\dagger+\mathbf{A}, \tag{17}$$

where

$$\mathbf{K}=\begin{pmatrix} \alpha_+ & \beta_+ \\ \beta_- & \alpha_- - ic\Delta k \end{pmatrix}, \quad \mathbf{A}=\begin{pmatrix} \mathscr{A}_{++} & \mathscr{A}_{+-} \\ \mathscr{A}_{-+} & \mathscr{A}_{--} \end{pmatrix}.$$

Here we allow for the characteristics of four-wave interaction associated with the phase-matching condition

$$(\mathbf{k}_+-\mathbf{k}_-+\mathbf{k}_{L-}-\mathbf{k}_{L+})\mathbf{r}=0, \tag{18}$$

which in the present geometry takes the form

$$(k_+-k_-)l+(k_{L-}-k_{L+})x=0. \tag{19}$$

In this equation, l is y or z, depending on the direction of photon propagation. One can see from this expression that the mismatch $\Delta k=k_+-k_-$ strongly affects the propagation of the scattered photons. Transforming from total to partial derivatives by means of the substitution $d/dt\to\partial/\partial t+c(\partial/\partial l)$, we find the steady-state solution of Eq. (17):

$$\Sigma=\exp(\bar{\mathbf{K}}L)\Sigma^{(0)}[\exp(\bar{\mathbf{K}}L)]^\dagger + \int_0^L \exp(\bar{\mathbf{K}}l)\,\bar{\mathbf{A}}\,[\exp(\bar{\mathbf{K}}l)]^\dagger\,dl, \tag{20}$$

where L is the transverse size of the atomic beam and $\bar{\mathbf{K}}=\mathbf{K}/c$. The first term in this expression describes the homogeneous solution, for which the vacuum states $\Sigma(0)=I/2$ can be taken as the initial condition. The propagation of the scattered radiation itself is described by the second term, which determines the quantity of interest, N_x. The details of the calculation of (20) can be found in Ref. 8. We find N_x by means of the computational method described above [see Eq. (15)].

Figure 3 displays the line profile S_x as a function of magnetic field strength (in the form of the parameter Ω/γ) for various pump-wave intensities and offsets of the pump wave from resonance for an optically thick (solid line, $\alpha_0 L=100$) and optically thin (dashed line, $\alpha_0 L\ll 1$) atomic beams with exact phase matching ($\Delta k=0$). Here α_0 is the unsaturated absorption coefficient of the radiation at line center ($E_\sigma=\Omega=\Delta_L=0$). For an optically thin atomic beam, the line profile S_x can be determined with the formula given by Avan and Cohen–Tannoudji [see Eq. (10)].

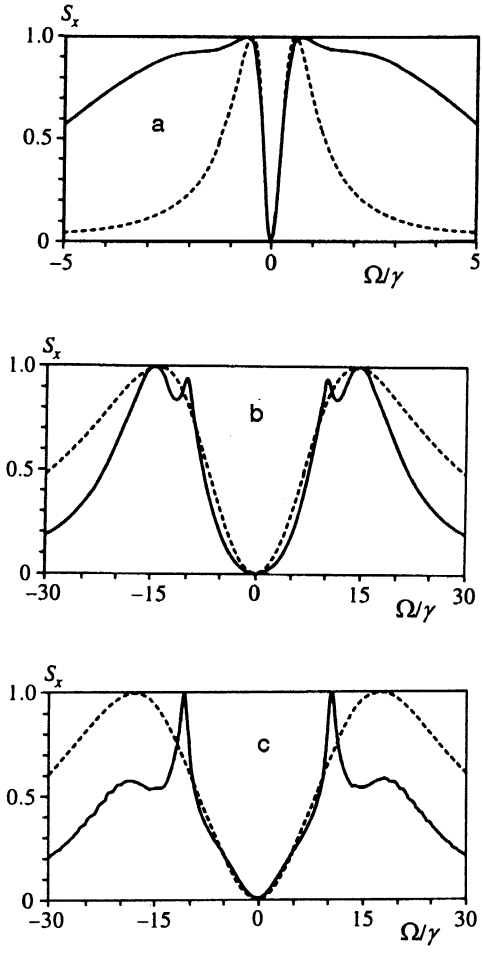

FIG. 3. S_x as a function of Ω (magnitude of the magnetic field) for scattering of the pump wave by optically thick (solid curve, $\alpha_0 L=100$) and optically thin (dashed curve, $\alpha_0 L\ll 1$) atomic beams with various parameters: a) $V/\gamma=0.1$, $\Delta_L=0$; b) $V/\gamma=10$, $\Delta_L=0$; c) $V/\gamma=10$, $\Delta_L/\gamma=10$. The peak values of S_x are normalized to unity.

One can see from Fig. 3 that propagation effects (stimulated processes) substantially change the line profile of the total Hanle signal. It is pointed out in Refs. 7 and 8 that in strong fields the inelastic component dominates the spectrum of the Hanle signal. Our analysis for an optically thick atomic beam shows that the total Hanle signal is then also determined by inelastic scattering, i.e., by N_x^{inel}. In weak fields, the elastic component is the dominant one. For the total Hanle signal, however, the ratio of the elastic and inelastic scattering contributions (correspondingly, the ratio between N_x^{el} and N_x^{inel}) in an optically thick medium depends strongly on the length of the medium. If the elastic component dominates for short lengths, then as the optical depth increases, N_x^{el} becomes of the order of N_x^{inel}, which is demonstrated in Fig. 4, and as the optical depth of the medium increases further, the inelastic scattering component N_x^{inel} becomes the dominant one. This effect can be tested experimentally relatively simply, and it makes it possible to investigate the effect of stimulated processes on the properties of the Hanle signal.

The effect of a phase mismatch on N_x is demonstrated in Fig. 5. As pointed out in Ref. 8, the formal calculation of

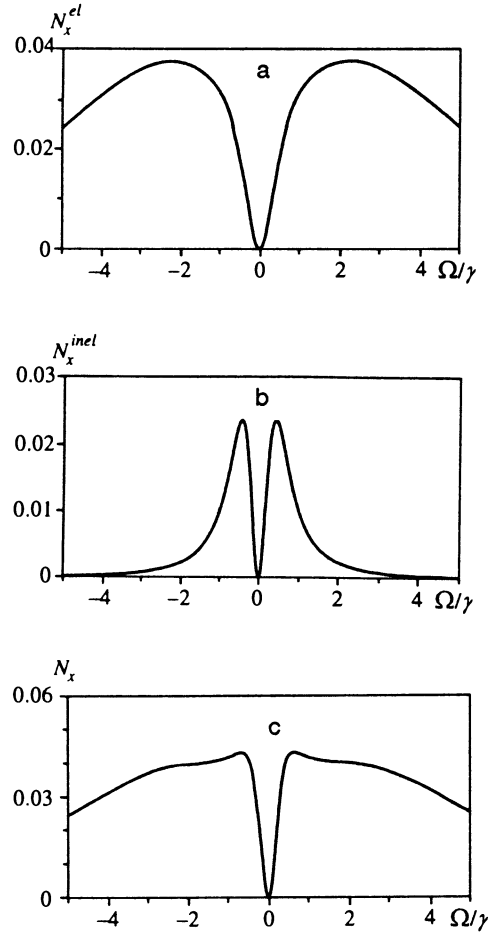

FIG. 4. N_x^{el} (a), N_x^{inel} (b), and N_x (c) as functions of Ω for $V/\gamma=0.1$, $\Delta_L=0$, $\alpha_0 L=100$, and $\Delta k=0$.

these plots for fixed $\Delta k \neq 0$ is an ill-posed problem, since the difference in the phase velocity of the waves leads to unphysical results in the limit $\Omega \to 0$. In the present work, the mismatch Δk is modeled by the expression

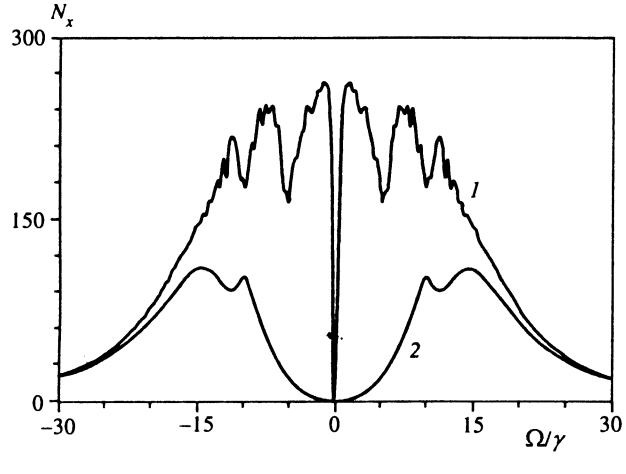

FIG. 5. N_x as a function of Ω for $V/\gamma=0.1$, $\Delta_L=0$, and $\alpha_0 L=100$. Curve *1* was constructed in the presence of a phase mismatch Δk given by Eq. (21), and curve *2* was constructed for $\Delta k=0$.

$$\Delta k=\frac{\chi\ \mathrm{Im}(\alpha_+-\alpha_-)}{\Omega^2+\gamma^2}. \tag{21}$$

This expression is not, in general, a solution of the dispersion relation for scattered waves (Eq. (45) in Ref. 8). A calculation of N_x using (21) is primarily illustrative. The constant χ in Eq. (21) was chosen by requiring that n_x be greatest maximum at the peaks of its spectral distribution, and that the function in the denominator of this expression also optimize Δk for various values of the magnetic field. One can see from Fig. 5 that the mismatch strongly influences not only the absolute value of N_x, but also its line profile. We call attention especially to the large change in the width of the dip in the line profile in the presence of a phase mismatch, while according to Fig. 3 for $\Delta k=0$ this width changes little as the optical depth of the medium increases. An experimental test of this effect could make it possible to clarify the role of four-wave mixing in the generation of the Hanle signal in optically thick media.

4. COMPARISON OF RESULTS FOR VOIGT AND FARADAY GEOMETRIES

The investigation presented above, and the results obtained in Refs. 7 and 8, refer to the properties of the scattered radiation, first, for the Voigt geometry (see Fig. 1) and second, perpendicular to the propagation direction of the pump wave. The polarization structure of the radiation scattered at an angle to the pump direction (neglecting thermal motion of the atoms) is governed by Eqs. (4) and (5). In Ref. 10 the scattered radiation was described in the Faraday geometry, i.e., with the magnetic field parallel to pump wave propagation. The equations for the scattered radiation are formally identical to the equations for the Voigt geometry. To obtain the polarization structure of the scattered radiation in the Faraday geometry, we interchange the x and z axes in Fig. 1: the magnetic field will then be directed along the z axis. Then Eqs. (4) and (5) will be the desired equations in this geometry as well. The distribution of the scattered radiation will therefore be identical in the two cases, to within a rotation of 90° about the y axis (this is associated with the rotation of the quantization axis).

The agreement obtained between the results (to within the indicated rotation) is not complete. The main difference arises in forward scattering, and is due to the differing interactions of the pump wave with the medium in these geometries. The Hamiltonians describing the interactions are formally identical, but the expansion of the initial wave into σ components has a different physical import. In the Faraday geometry these are left- and right-hand circularly polarized waves, while in the Voigt geometry they are linearly polarized waves. Their effect on the atoms is the same, however: they excite σ transitions of the atoms *in like manner*. Only the spatial orientations of the dipoles are different. The agreement between the scattering results is therefore understandable.

We now consider forward scattering. In Ref. 10 it is shown that in the Faraday geometry, correlation functions $\langle a^+_{\sigma k} a^+_{\sigma' \tilde{k}}\rangle$ and $\langle a_{\sigma k} a_{\sigma' \tilde{k}}\rangle$ arise, which correspond to four-wave mixing in the forward direction:

$$\mathbf{k}_{L\sigma}+\mathbf{k}_{L\sigma'}=\mathbf{k}_{\sigma}+\bar{\mathbf{k}}_{\sigma'}. \tag{22}$$

Four-wave mixing can be implemented for photons with either the same or different polarizations, and the process is nondegenerate: $2\omega_L=\omega+\bar{\omega}$, where ω and $\bar{\omega}$ are the frequencies of photons with wave vectors $\mathbf{k}_\sigma$ and $\bar{\mathbf{k}}_\sigma$, respectively. The dynamics of the scattered radiation is described by the system of equations (18) in Ref. 10. These equations also describe forward scattering in the Voigt geometry, but the sense of the operators a_σ (a_σ^+) is different. Whereas in the Faraday geometry they describe annihilation (creation) of circularly polarized photons—left- or right-hand polarization—in the Voigt geometry they describe only linear polarization identical with the polarization of the pump wave, and they differ only in their interactions with the atomic transitions. In the latter case, no scattered radiation polarized orthogonally with respect to the polarization of the pump wave appears in the forward direction [see Eq. (6)], while in the Faraday geometry it does arise and is described by Eq. (2). We call it the Hanle signal $S_x^{ph}\propto N_x$ in the forward direction. Then the total signal is

$$S_x=S_x^{ph}+S_x^L, \tag{23}$$

where S_x^L comes from the change in polarization properties of the pump wave as it passes through the medium. This change arises for two reasons: the well-known rotation of the polarization plane resulting from the differing dispersion of left- and right-hand polarized waves, and the differing absorption of these waves. Since $S_x^L\propto I_x=|E_+-E_-|^2$, it follows from Maxwell's equations for the slowly varying amplitudes that

$$\frac{\partial I_x}{\partial z}=\mathscr{P}_x^*(E_+-E_-)+c.\ c., \tag{24}$$

where $\mathscr{P}_x \propto i(\mu_{0+}\rho_{+0}-\mu_{0-}\rho_{-0})$. In the optically thin case, $E_+-E_- \propto \mathscr{P}_x$. Then

$$I_x\propto|\mu_{0+}\rho_{+0}-\mu_{0-}\rho_{-0}|^2L,$$

or

$$S_x^L\propto|\mu_{0+}\rho_{+0}-\mu_{0-}\rho_{-0}|^2. \tag{25}$$

Comparing this with Eq. (16) for $\mathscr{A}_x^{\mathrm{el}}$, we note that the basic dependences (on the magnetic field strength, the pump power, and the pump offset from resonance) are the same. The quantity $\mathscr{A}_x^{\mathrm{el}}$ was investigated in Ref. 7. We point out that exactly at resonance ($\Delta_L=0$), the left- and right-hand S_x^L polarized waves are absorbed identically, and

$$S_x^L\propto(\mathrm{Im}\mathscr{P}_x)^2\propto\varphi^2, \tag{26}$$

where φ is the angle by which the plane of polarization is rotated. This has been investigated in the strong-field case.[10]

We also note that the scattering of an intense ($V\geqslant\gamma$) pump in an optically thick medium is likely to produce a spectral–angular instability of the pump wave. This instability is accompanied by the generation of conical radiation (reviewed in Ref. 13), and is described by Eqs. (18) in Ref. 10.

Finally, we mention that for the (axisymmetric) Faraday geometry, the polarization vector of the pump wave can be arbitrarily oriented in the xy plane with axes fixed . Moreover, the foregoing description holds for an arbitrarily polarized pump, i.e., it may be that $|E_+|=|E_-|$. In contrast, the Voigt geometry does not possess this symmetry, and the corresponding results hold only for the situation displayed in Fig. 1. If, however, the pump wave is polarized at some angle to the y axis, then our description will no longer be correct, since the field will then have a nonvanishing z component that will induce π transitions. The description of the structure of the scattered radiation will also change: in addition to the operators a_σ, we also have operators a_π, along with the corresponding correlation functions $\langle a_\pi^+ a_\pi\rangle$, $\langle a_\pi^+ a_\sigma\rangle$, and $\langle a_\sigma^+ a_\pi\rangle$.

5. CHARACTERISTICS OF THE HANLE EFFECT FOR THE $J=1\rightarrow J=0$ TRANSITION

The approach developed in Refs. 7, 8, and 10 to describe the resonance scattering of a monochromatic wave is a general approach when viewed in terms of the structure of the scattered radiation. Actual results depend on the form of the A and B coefficients, which are determined by the properties of the medium. In both the present work and in Refs. 7, 8, and 10, an interaction with the $J=0\rightarrow J=1$ transition was investigated, involving a V-type interaction between the radiation and atoms.

To extend these results to resonant scattering of a wave involving transitions with arbitrary angular momentum in the upper and lower states, it is of interest to investigate the Λ-type configuration pertinent to the $J=1\rightarrow J=0$ transition. Our analysis of the scattering of a monochromatic wave in this transition (the computational details will be published in a forthcoming paper) shows that the characteristics of the scattered radiation are substantially different from the results obtained for the $J=0\rightarrow J=1$ transition. This has primarily to do with spontaneous sources for the correlation functions $\langle a_\sigma^+ a_{\sigma'}\rangle$, which describe interference processes:

$$\int \mathscr{A}_{\sigma\sigma'}\,d\nu=0 \quad (\sigma\neq\sigma'), \tag{27}$$

$$\int \mathscr{A}_{\sigma\sigma}\,d\nu \propto \rho_{00}. \tag{28}$$

where ρ_{00} is the population of the upper state (with $J=0$). These expressions differ from the expressions (9) for the $J=0\rightarrow J=1$ transition. The condition (27) shows that there are no interference effects (for example, level crossing with $\Omega=0$) in the total intensity of the scattered radiation for an optically thick medium with a $J=1\rightarrow J=0$ working transition, since quantum mechanics tells us that processes with the same final states interfere with one another. For example, in a $J=0\rightarrow J=1$ transition, the scattered σ waves transfer an atom into a single lower state with $m_J=0$, whereas for a $J=1\rightarrow J=0$ transition, they transfer an atom into different states with $m_J=\pm1$. In an optically thick medium, the spectra of the scattered radiation are altered by stimulated processes. It should therefore be expected that the total (integrated) contribution of interference terms to the Hanle signal for the $J=1\rightarrow J=0$ transition will be nonvanishing.

The Hanle effect for the $J=1\rightarrow J=0$ transition can be investigated experimentally in the case of laser light scattering by the excited states of inert-gas atoms. The scattering of laser radiation by the excited states of neon was recently studied experimentally in Ref. 5 for this transition in the Faraday geometry. The investigation was performed for exact resonance between the incident wave and the transition frequency and for relatively low (nonsaturating) values of the intensity, and it focused mainly on the orthogonally polarized radiation scattered in the direction of propagation of the pump wave. A halo, reminiscent of the well-known conical radiation, was detected around the main beam in the transverse distribution of the scattered radiation.[13] The strength of the magnetic field was such that the Zeeman splitting was greater than the linewidth.

It follows from the investigation in Sec. 4 of the present paper that the experimentally recorded signal will be determined by the expression (23). In an optically thin medium, which corresponds to the conditions of the experiment being discussed, the signal will be determined by S_x^L. The contribution of S_x^{ph} will be small in this case, since it is determined by the fluorescence within a small solid angle. This is supported by the fact that in the present case, no displaced Zeeman components were observed experimentally in the total signal. The signal S_x^L due to exact resonance between the pump wave and the transition frequency will be determined by (26). To explain the experimental results, Junger *et al.*[5] employ a similar expression that takes account of thermal motion of the atoms and the transverse Gaussian intensity distribution of the pump wave. The theoretical calculations agree well with the experimental data. We assume that this is a faithful model that can be used to interpret the experimental results.

In comparing the ring-shaped structure obtained in their experiments with the conical radiation,[13] however, Junger *et al.* point out that conical radiation was usually generated in very strong fields, while their experiment involved weak fields. They conclude that the difference between these phenomena is basically due to the different degree of nonlinearity in the corresponding processes. We believe that this is not entirely correct, since these phenomena correspond to different physical processes: the formation of the ring-shaped structure of the scattered radiation in Ref. 5 is associated with the rotation of the polarization plane of the pump wave (taking into consideration its nonuniformity over the cross section of the beam), and is described by the quantity S_x^L in Eq. (23), while the conical radiation is determined by the parametric amplification and four-wave mixing of fluorescence photons[14] and is described by the quantity S_x^{ph} in Eq. (23). Noted that Cherenkov radiation can influence the initial development of spectral–angular instability of the laser wave in a resonant medium,[15] but the developed stage of this instability, which, in general, determines the conical radiation, is mainly due to parametric and four-wave processes. We also point out that according to the theory of resonant four-wave mixing,[16,17] instability of nonsaturating fields can also be observed.

In summary, the decisive role of S_x^L in the formation of the signal investigated in Ref. 5 is associated with the small optical depth of the medium ($\alpha_0 L \ll 1$). As $\alpha_0 L$ increases, the contribution of S_x^{ph} increases, and S_x^L can even vanish, which is equivalent to rotation of the polarization plane by $2\pi m$, where m is an integer.

One of the authors, A.P., expressed his gratitude to the Russian Fund for Fundamental Research (Grant No. 9-02-05853) and to the International Research Foundation (Grant RLT 300) for supporting this work.

[1] W. Hanle, Z. Phys. **30**, 93 (1924).
[2] Z. Phys. D **18** (1991) (issue in honor of the ninetieth anniversary of Hanle's birth).
[3] E. B. Aleksandrov, G. I. Khvostenko, and M. P. Chaĭka, *Interference of Atomic States* [in Russian], Nauka, Moscow (1991).
[4] G. Vemuri, M. H. Anderson, J. Cooper *et al.*, Phys. Rev. A **44**, 2217 (1991).
[5] P. Junger, A. Lindberg, and B. Stahlberg, Phys. Rev. A **44**, 1369 (1993).
[6] E. Landi Degl'Innocenti, Solar Phys. **85**, 3 (1983); *ibid.*, **91**, 1 (1984).
[7] F. A. Lomaya and A. A. Panteleev, Zh. Éksp. Teor. Fiz. **103**, 1970 (1993) [JETP **76**, 976 (1993)].
[8] F. A. Lomaya and A. A. Panteleev, Zh. Éksp. Teor. Fiz. **106**, 886 (1993) [JETP **79**, 486 (1994)].
[9] B. R. Mollow, Phys. Rev. **188**, 1969 (1969).
[10] A. A. Panteleev, Zh. Éksp. Teor. Fiz. **99**, 1684 (1991) [Sov. Phys. JETP **72**, 939 (1991)].
[11] M. O. Scully and W. E. Lamb, Jr., Phys. Rev. **159**, 208 (1967).
[12] P. Avan and C. Cohen-Tannoudji, J. de Phys. Lett. **36**, L85 (1975).
[13] N. B. Abraham and W. J. Firth, J. Opt. Soc. Am. B **7**, 951 (1990).
[14] G. S. Agarval and R. W. Boyd, Phys. Rev. A **38**, 4019 (1988).
[15] L. You, J. Mostowski, and J. Cooper, Phys. Rev. A **46**, 2903 (1992); ibid., **46**, 2925 (1992).
[16] T. Fu and M. Sargent III, Opt. Lett. **4**, 366 (1979).
[17] D. J. Harter and R. W. Boyd, IEEE **QE-16**, 1126 (1980).

Translated by M. E. Alferieff